Charge transfer and fluctuations in deep-inelastic electroproduction*

J. L. Newmeyer and Dennis Sivers
Stanford Linear Accelerator Center, Stanford University, Stanford, California 94305
(Received 25 February 1974)

We consider what can be learned about the nature of electroproduction from a measurement of the charge transferred across a surface in momentum space in the hadronic final state. The mean charge transfer as a function of rapidity, $\langle u(y)\rangle$, can be used to test quark-parton assumptions. The mean square charge transfer, $\langle u^2(y)\rangle$, can be measured and compared with an inclusive single-particle distribution in order to explore the possibility of new types of clustering effects in the current fragmentation region.

I. INTRODUCTION

The success of the quark-parton model in describing deep-inelastic electroproduction[1] must now be weighed against the inability of simple versions of the model to adequately describe new data on e^+e^- annihilation.[2] The question of whether we need to accept partons as a necessary feature of models for deep-inelastic processes deserves further careful study. One approach to this question involves making a detailed phenomenological study of the hadronic final states of electroproduction and comparing with parton-model predictions. Knowledge of the final state allows us to test parton-model assumptions and come to grips with fundamental dynamical questions.

There already exists a substantial body of literature[1,3] dealing with the inclusive process $\gamma^*(-q^2)N \to h_i$ + (anything); this work represents an important first step in the study of electroproduction processes in that it shows that the data at this level are roughly consistent with quark-parton ideas. Our intention here is to take another step and develop a class of simple one-dimensional models for the *exclusive* process $\gamma^*(-q^2)N \to h_1 \cdots h_n$. These models are patterned after multiperipheral[4] or multiperipheral-cluster[5] models for hadronic production processes. We demonstrate a simple way of handling quantum numbers which enables us to reproduce some of the standard quark-parton-model results for multiplicities and inclusive-particle ratios.

As an example of the type of calculations possible with a model for the exclusive electroproduction processes, we discuss predictions of the mean-square charge transfer across a given rapidity, $\langle u^2(y)\rangle$. This measurement has been shown, in hadronic collisions, to provide a sensitive test of the clustering properties of the final-state hadrons.[6,7] In particular, it can resolve the alternatives of short-range order and of diffractive fragmentation. Similarly, we argued in a previous paper[8] that measurement of $\langle u^2(y)\rangle$ is capable of deciding between an underlying parton approach to e^+e^- annihilation and a generalized vector dominance or "statistical fireball" mechanism. Mueller-Regge analysis suggests that in the different kinematic regions in deep-inelastic electroproduction, dynamic properties appropriate to purely hadronic systems as well as those peculiar to current processes will be present and can be sampled.[9] Any deviation from the empirical result[6]

$$\langle u^2(y)\rangle \cong 0.8\, d\sigma^{\rm ch}_{(1)}/dy \tag{1.1}$$

valid in hadronic production can be interpreted as evidence for a qualitatively new clustering mechanism in deep-inelastic phenomena.

The plan of this paper is as follows: In Sec. II we assemble, for convenience, the kinematic formulas relevant for the discussion of the deep-inelastic electroproduction of a specific exclusive channel. We then present the kinematic simplifications due to the assumption of limited transverse momenta of the produced hadrons and introduce the definitions of the charge-transfer measurables.

In Sec. III we introduce the one-dimensional multiperipheral quark-line model which provides our basic calculational tool and demonstrate its connection to the conventional quark-parton models by calculating charged-particle ratios, charge transfer, and charge density.

In Sec. IV we discuss $\langle u^2(y)\rangle$ from both a simple multiperipheral viewpoint and a cluster-multiperipheral viewpoint; we also touch upon the use of this quantity in assessing the validity of a correspondence principle conjectured by Bjorken and Kogut.[10] Section V summarizes and presents our conclusions.

II. DEFINITIONS AND CONVENTIONS

In this section we briefly review the kinematics for the deep-inelastic electroproduction of hadrons. We intend to establish the terminology appropriate for the definition and measurement of charge transfer moments and will not deal here with model calculations.

The exclusive process $eN \to eh_1 \cdots h_n$ and variables relevant to its description in the one-photon approximation are depicted in Fig. 1. The differential cross section averaged over initial spins and summed over final spins is given by[11]

$$\frac{d\sigma_n}{d\Omega\, dE'\, d\Gamma_n} = \kappa\left[\sum_{\mu\nu} \rho_{\mu\nu}\, \frac{d\sigma_n^{\mu\nu}}{d\Gamma_n}\right], \tag{2.1}$$

with virtual-photon flux factor

$$\kappa = -\frac{\alpha(\nu + q^2/2m)E'}{4\pi^2 q^2 E}\left(\frac{2}{1-\epsilon}\right) \tag{2.2}$$

and photon polarization and spin three-vector

$$\epsilon = \frac{4EE' + q^2}{2E^2 + 2E'^2 - q^2}, \tag{2.3}$$

$$s^{\pm} = \left\{\left[\tfrac{1}{2}(1+\epsilon)\right]^{1/2}, \pm i\left[\tfrac{1}{2}(1-\epsilon)\right]^{1/2}, (q/\nu)\epsilon^{1/2}\right\}.$$

In the laboratory frame the polarization density matrix of the virtual photon is given, using gauge invariance, by

$$\rho_{\text{lab}} = \begin{bmatrix} \frac{1+\epsilon}{2} & 0 & \frac{q}{\nu}\left[\frac{\epsilon(1+\epsilon)}{2}\right]^{1/2} \\ 0 & \frac{1-\epsilon}{2} & 0 \\ \frac{q}{\nu}\left[\frac{\epsilon(1-\epsilon)}{2}\right]^{1/2} & 0 & \left(\frac{q}{\nu}\right)^2\epsilon \end{bmatrix}. \tag{2.4}$$

The virtual-photon–nucleon cross section for the process $\gamma^*(-q^2)N \to h_1 \cdots h_n$ is

$$\frac{d\sigma_n^{\mu\nu}}{d\Gamma_n} = \frac{d^{3n}\sigma^{\mu\nu}(\nu, q^2; \vec{p}_1 \cdots \vec{p}_n)}{d^3p_1/E_1 \cdots d^3p_n/E_n}. \tag{2.5}$$

In what follows we will assume that hadrons are produced with limited momenta transverse to the direction of the virtual photon.[12] In the lab frame with longitudinal axis along this direction we therefore integrate over the transverse momenta of produced hadrons. The azimuthal integration wipes out interference between transversely and longitudinally polarized photons, leaving us with

$$\frac{d\sigma_n}{d\Omega\, dE'\, dy_1 \cdots dy_n} = \kappa\left(\frac{d\sigma_n^T}{dy_1 \cdots dy_n} + \epsilon\, \frac{d\sigma_n^L}{dy_1 \cdots dy_n}\right), \tag{2.6}$$

where $y_i = \sinh^{-1}(p_{Li}/m_{Ti})$ is the laboratory rapidity of hadron h_i and $m_{Ti} = (m_i^2 + \langle p_{Ti}\rangle^2)^{1/2}$ is its average transverse mass.

It will often be convenient to make use of the empirical result[13]

$$\sigma_{\text{tot}}^L(\nu, q^2) \lesssim 0.2\, \sigma_{\text{tot}}^T(\nu, q^2) \tag{2.7}$$

and refer to model calculations of the cross sections for a transversely polarized photon. In each case, however, our arguments can be repeated for longitudinally polarized photons and the two results combined using (2.6) to produce the complete result for the final state in electroproduction. We shall usually drop the label T for convenience.

Based on the dynamical assumptions of the parton model[9] or on a Mueller-Regge analysis[14] of the inclusive process $\gamma^*(q)N \to h_i X$ the phase space available to each particle is customarily divided into five distinct regions, as depicted schematically in Fig. 2:

(1) nucleon fragmentation region (NFR),

$$y_i \in (y_{\min}, y_{\min} + \xi_1), \quad \xi_1 \text{ finite};$$

(2) hadronic plateau (HP),

$$y_i \in (y_{\min} + \xi_1, \ln\omega + \xi_2), \quad \xi_1, \xi_2 \text{ finite};$$

(3) hole fragmentation region (HFR),

$$y_i \in (\ln\omega + \xi_2, \ln\omega + \xi_3), \quad \xi_2, \xi_3 \text{ finite};$$

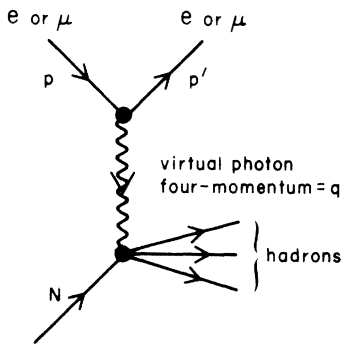

$q^2 < 0$

$\nu = q^0 = p^0_{\text{lab}} - p^{0\prime}_{\text{lab}}$

$K = \nu + q^2/2M$

$s = W^2 = 2M\nu + M^2 + q^2$

$\omega = -2M\nu/q^2$

FIG. 1. Kinematics of an exclusive electroproduction channel in the one-photon limit.

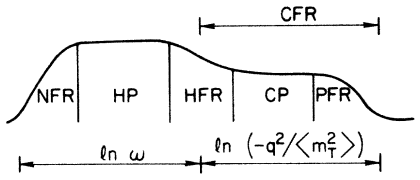

FIG. 2. Kinematic regions in rapidity space for the final-state hadrons deduced from Mueller-Regge analysis or from parton-model assumptions. From left to right, slow to fast in the lab frame: nucleon fragmentation region (NFR), hadron plateau (HP), hole fragmentation region (HFR), current plateau (CP), parton fragmentation region (PFR). The last three regions are sometimes lumped together as the current fragmentation region (CFR).

(4) current plateau (CP),

$y_i \in (\ln\omega + \xi_3, y_{\max} - \xi_4)$, ξ_3, ξ_4 finite;

(5) parton fragmentation region (PFR),

$y_i \in (y_{\max} - \xi_4, y_{\max})$, ξ_4 finite;

here $y_{\min} \cong \ln(m_T/m_N)$ and $y_{\max} \cong \ln(s/m_T^2) + \ln(m_T/m_N)$. The labels on the regions reflect the dynamical suggestion of the parton picture, but they may be taken as conventional.[9] The last three regions in the above are collectively referred to as the current fragmentation region (CFR). The hadronic regions have length in rapidity space $Y_h \cong \ln\omega$, and the CFR has a length $Y_c \cong \ln[-q^2/(m_T^2)]$, with $Y = y_{\max} - y_{\min} \cong Y_h + Y_c$. The specific implication of the parton model is that the dynamics of these regions can be quite distinct. Since partons represent the fundamental charged constituents of hadrons it is our suggestion here that such discontinuities in the dynamics should be reflected in the structure of charge-transfer measurements as we vary the rapidity, y, across the different kinematical regions in Fig. 2. We surmise that this might be true even for cases with q^2 and ω too small for the plateau regions to develop. There is already some hint from measurements of charge ratios in the parton fragmentation region that the charge-transfer properties of the final state in electroproduction may be different from those found in purely hadronic interactions.[3,15]

Now let us consider briefly the definitions of the various moments of charge transfer. For a given n-particle final state we label the particles so that the rapidities are ordered, $y_i < y_{i+1}$. The *charge transfer across rapidity* y in an event is defined as

$$u(y) = Q_N - \sum_{y_i < y} Q_i = \sum_{y_j > y} Q_j \,, \tag{2.8}$$

where Q_N is the charge of the target nucleon. The average charge transfer in the n-particle final state is given by

$$\langle u(y)\rangle_n = \sigma_n^{-1} \int dy_1 \cdots dy_n \, \frac{d\sigma}{dy_1 \cdots dy_n} \, u(y) \,, \tag{2.9}$$

where $u(y)$ in the integrand is understood to be an implicit function of the rapidities, y_i, of the final-state particles. We will also consider the inclusive charge transfer

$$\langle u(y)\rangle = \sigma_{\text{tot}}^{-1} \sum \langle u(y)\rangle_n \sigma_n \,. \tag{2.10}$$

This is related to single-particle inclusive densities as follows: By weighting the inclusive density for the process $\gamma^*(-q^2)N \to h_c(y)X$ by the charge of hadron c we can form the *inclusive charge density:*

$$\frac{d\langle Q\rangle}{dy} = \sum_c Q_c \left(\frac{d\sigma}{dy}\right)_{\gamma^* N \to c} (\omega, q^2; y) \,. \tag{2.11}$$

Using charge conservation, (2.10) and (2.11) can be related:

$$\langle u(y)\rangle = Q_N - \int_{y_{\min}}^{y} \frac{d\langle Q\rangle}{dy'} \, dy' \,. \tag{2.12}$$

Although we will deal here with charge transfer, we could obviously study the transfer of any other additive quantum number (such as strangeness or baryon number) by making the appropriate changes in (2.8)–(2.12). The use of rapidity in these definitions is only a convention. We could equally well define the charge transfer across a given value of p_L or across a given value of Feynman's scaling parameter, $z = p_L/p_{L\max}$. Because of the limited transverse momenta, the ordering is unaltered in the high-energy limit, $y_i < y_{i+1} \rightleftarrows z_i < z_{i+1}$, and it is simple to change from one set of variables to the other. For convenience of notation, however, we will stick with rapidities.

Also of crucial importance in our discussion will be the second moments of the charge transfer, $\langle u^2(y)\rangle_n$ and $\langle u^2(y)\rangle$,

$$\langle u^2(y)\rangle_n = \sigma_n^{-1} \int dy_1 \cdots dy_n \, \frac{d\sigma}{dy_1 \cdots dy_n} [u(y)]^2 \,, \tag{2.13}$$

$$\langle u^2(y)\rangle = \sigma_{\text{tot}}^{-1} \sum_n \sigma_n \langle u^2(y)\rangle_n \,. \tag{2.14}$$

These simple measurements are sensitive to the clustering properties of the final-state hadrons. In hadronic collisions they can be used to distinguish between multiperipheral and fragmenta-

tion models.[7] In e^+e^- annihilations these measurements have been shown capable of resolving the difference between an underlying parton structure and a statistical or fireball approach to the dynamics of the annihilation process.[8]

We believe that the charge-transfer measurements (2.9), (2.10), (2.13), and (2.14) will serve a useful role in understanding electroproduction, and we now turn to some model calculations to illustrate their potential.

III. CHARGE TRANSFER AND AN EXCLUSIVE QUARK-PARTON MODEL

The parton model is usually formulated to describe inclusive processes.[3] For example, the approximate shape of the inclusive differential cross section for $\gamma^*(-q^2)N \to h(y)X$ illustrated in Fig. 2 is simple to obtain from parton-model assumptions.[9] For our purposes, however, it is convenient to have a model for the various possible exclusive processes which embodies quark-parton ideas. To accomplish this we can interpret the diagram in Fig. 2 as giving the density of an analog one-dimensional classical gas. We then utilize the identification of multiperipheral models in the strong-ordered limit with a one-dimensional nearest-neighbor gas[16] to suggest the existence of a multiperipheral description of the $2 \to n$ amplitude.

The quark-parton substructure of our model, for exclusive processes, will be inserted by constructing the framework of our multiperipheral diagrams from quark lines as shown in Fig. 3. One quark line in this diagram is selected to play a special role as it couples to the photon. In order to absorb the large spacelike momentum of the photon, this line approximately "spans" the photon fragmentation region, winding up in the leading hadron. Other quark lines are constrained only to the extent that they must terminate in the target or in final-state hadrons. To remind us further of the possibility for distinct dynamics in the hadronic regions (NFR and HP) and the current regions (HFR, CP, and PFR), the diagrams in Fig. 3 are drawn with straight lines in the hadronic sector and curved lines in the current sector. This distinction may not, of course, be necessary. One of the possibilities that we would like to consider is based on the suggestion by Bjorken and Kogut[10] of *correspondence*, that is, that the basic features of the normalized cross sections do not depend significantly on $(-q^2)$ at fixed s. We will examine this concept more carefully later.

The diagrams in Fig. 3 bear strong resemblance to Harari-Rosner duality diagrams.[17] We do not,

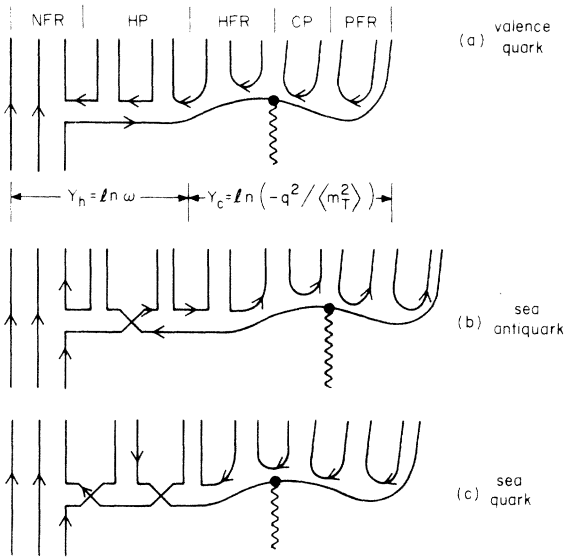

FIG. 3. Quark line diagrams indicating schematically the production of hadrons in the various kinematic regions. Diagram (a) shows the photon coupling to a valence quark, one of the three quarks in the target nucleon. In diagram (b) the quark line coupled to the photon terminates in one of the hadrons in the multiperipheral chain. In parton-model language it is a "sea antiquark." Diagram (c) illustrates the coupling of the photon to a "sea quark." Not shown, but possible, are diagrams with nonexotic baryon exchange along the multiperipheral chain.

however, want necessarily to adopt the trappings of dual models here; the connection has been studied elsewhere in the Mueller-Regge framework.[3,18] In particular we do not adopt the criteria of exchange-degeneracy patterns implied by resonance saturation of various discontinuities, and in contrast with dual modelists we do not attach any special significance to planar diagrams. We are not interested in early scaling criteria obtained from interpreting separately diagrams with twists among quark lines. Our goals are more modest; the quark lines in our figure merely illustrate possible quantum-number flow in a nearest-neighbor multiperipheral model.

Some remarks are in order concerning certain general features of the physical process that we do want Fig. 3 to reflect. The multiperipheral-type graphs consist of valence-parton lines (those originating or terminating in the target nucleon) and sea-parton lines (all others). For example, Figs. 3(a), 3(b), and 3(c) show a virtual photon striking a valence quark, a sea antiquark, and a sea quark, respectively. The diagram in the current-fragmentation region (CFR) cannot be identified with a multiperipheral chain in the traditional sense, even though it has the multi-

peripheral ordering, since momentum transfers are not necessarily small. The struck parton ends up in the leading meson, and in the usual parton language the phase space between $y = Y_h$ and $y = y_{max}$ is filled by parton-antiparton pairs which condense to hadrons. The hadronic leading-particle effect is implemented by assuming that the remnant of the nucleon usually becomes the trailing particle. For simplicity the diagrams are drawn as if all secondary particles are mesons or meson resonances. It is a simple modification to draw diagrams with baryon-antibaryon pairs produced in the final state and to include baryon exchange so that the leftmost particle is not necessarily a baryon.

Finally, some statement about the relationship between the strong-ordering assumption and interference effects is called for. For the annihilation process considered in Ref. 8, the strong-ordering assumption that the rapidity ordering of the final-state particles duplicates the ordering in the diagrams implies that there is at most one diagram that could be associated with any specified final state, hence the absence of interference. Therefore, the diagrams could be used directly to calculate probabilities rather than just amplitudes. For electroproduction it is not true that any specific final state has at most one diagram associated with it; both diagrams in Fig. 4 result in the same final state, for example. Unfortunately, dealing with probabilities is the limit of our model's sophistication, and we shall assume for the remainder of this paper that such interferences, when they occur, are negligible. We maintain the crucial strong-ordering assumption, as suggested by the appearance of our multiperipheral-like quark-line diagrams.

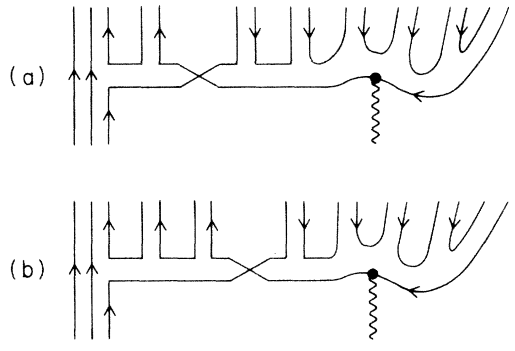

FIG. 4. Both of these diagrams can have the same ordering of particles in the final state. Given a specific model for vertex functions, propagators, etc., these diagrams could give different amplitudes, and we would have to consider their interference in order to calculate cross sections. In what follows we will always assume that a diagram can be associated with a probability—that is, each of our diagrams will represent a class of diagrams having the same ordering of final-state particles and we assume we have summed all such amplitudes and squared to produce the probability.

We now discuss a few explicit predictions of this model with an aim of showing the consistency of our model with many others, and of fixing some relevant parameters by comparing with data. We first consider two things which can be calculated without reference to exclusive final states, namely, charge ratios (e.g., π^+/π^-) for the leading (PFR) particles and inclusive charge density $d\langle Q\rangle/dy$ and transfer $\langle u(y)\rangle$; these can be determined as well in a Mueller-Regge picture. Then we shall treat the higher moment $\langle u^2(y)\rangle$ and $\langle u^2(y)\rangle_n$, all of which require knowledge of the exclusive final states.

A. Particle ratios at y_{max}

As a simple example of the use of a diagram such as Fig. 3, let us consider a calculation of the ratio of π^+ to π^- production near $y = y_{max}$ off of proton and neutron targets.[3,15] We make the usual identification of the quark content of the particles, e.g.,

$$\begin{aligned} &\pi^+ = (u\bar{d}), \quad p = (uud), \\ &\pi^- = (d\bar{u}), \quad n = (udd), \end{aligned} \tag{3.1}$$

and we assume, as mentioned previously, that the strong-ordering limit allows us to neglect interference effects and deal with probabilities. In the diagram of Fig. 3 we will label the quark (or antiquark) which couples to the photon as a (or $\bar{a}$). The coupling is proportional to $Q_a{}^2$. The photon strikes a quark in HFR near $y = Y_h$ and that quark winds up in the rightmost particle in the diagram. The ratio of the probability that this rightmost particle is π^+ to the probability that it is a π^- is then

$$R(\pi^+/\pi^-)\big|_{y=y_{max}} = \frac{Q_u{}^2\rho_u(Y_h) + Q_{\bar{d}}{}^2\rho_{\bar{d}}(Y_h)}{Q_{\bar{u}}{}^2\rho_{\bar{u}}(Y_h) + Q_d{}^2\rho_d(Y_h)}, \tag{3.2}$$

where $\rho_a(Y_h)$ is the probability (not probability *density*) that a parton line of type a is present at rapidity $y = Y_h$ (the location of HFR in our diagram) and we have assumed isospin and charge invariance of the current plateau (CP) in the sense that the *other* quark in the leading pion is taken from a sea having equal numbers of u, d, $\bar{u}$, and $\bar{d}$ quarks. The assumption that the quark coupled to the photon ends up in the rightmost pion corresponds to a constraint on the usual "parton fragmentation functions" at or near $y = y_{max}$. This assumption is reasonable in view of our picture of the current fragmentation being filled up by vacuum polarization of quark-antiquark pairs. If

the rightmost hadron in Fig. 3 is not a pion but an unstable resonance which decays statistically, then (3.2) requires some trivial modification. We do not want to deal further with clustering at this point since a discussion can be found in Sec. IV.

The probabilities $\rho_a(Y_h)$ are, strictly speaking, functions of the number and type of final-state particles with $y_i < Y_h$. When this number, n_h, is small, there is a large probability that the quark in question is a valence one coming from the target proton, and when it is large the memory of the quark content of the target particle vanishes. We note in passing that we can recover lost information if we have a complete description of the particles with $y_i < Y_h$. Even a partial reconstruction is useful; for example, $\gamma^* p \to \Delta^{++} h_2 \cdots h_n$ should have $R(\pi^+/\pi^-)|_{y \cong y_{\max}} < 1$.

After averaging over n_h with $Y_h \approx \ln\omega$ fixed the model is constructed to reproduce the decomposition of the probabilities into "valence" and "sea" components similar to the decomposition of the probability densities in the usual parton model. For a proton target we write

$$\begin{aligned}
&\rho_u(Y_h) = 2v_u(Y_h) + s(Y_h),\\
&\rho_d(Y_h) = v_d(Y_h) + s(Y_h),\\
&\rho_{\bar{u}}(Y_h) = \rho_{\bar{d}}(Y_h) = s(Y_h),\\
&\rho_s(Y_h) = \rho_{\bar{s}}(Y_h) = s'(Y_h),
\end{aligned} \tag{3.3}$$

where $v_d(Y_h)$, say, is the probability that a d-type valence quark of the proton will pass through $y = Y_h$, $s(Y_h)$ is the probability that a nonstrange quark (or antiquark) from the sea will be present, and $s'(Y_h)$ is the probability for a strange quark or antiquark from the sea. Note that isospin and charge conjugation invariance of the sea is assumed in (3.3), and the possibility of SU(3) breaking is allowed for by $s(Y_h) \neq s'(Y_h)$. To obtain the equivalent to (3.3) for a neutron target, one uses isospin invariance and simply interchanges the subscripts u and d. We then find from (3.2) and (3.3) that

$$\begin{aligned}
R^p(\pi^+/\pi^-)|_{y=y_{\max}} &= \frac{8v_u(Y_h) + 5\,s(Y_h)}{v_d(Y_h) + 5\,s(Y_h)},\\
R^n(\pi^+/\pi^-)|_{y=y_{\max}} &= \frac{4v_d(Y_h) + 5\,s(Y_h)}{2v_u(Y_h) + 5\,s(Y_h)}
\end{aligned} \tag{3.4}$$

for proton and neutron targets, respectively. It is noteworthy that for large ω, where $v_u(Y_h)$ and $v_d(Y_h)$ presumably become negligible, $R \to 1$ for both proton and neutron targets. For smaller ω the exact behaviors of $v_u(Y_h)$ and $v_d(Y_h)$ are important. We now consider how these densities can be determined independently from other measurements.

B. Inclusive charge density and charge transfer

Consider the shape of the charge transfer $\langle u(y)\rangle$ in the various kinematic regions. Based on quite general Mueller-Regge arguments or on direct examination of diagrams such as Fig. 3, the charge-transfer properties of electroproduction for $y < Y_h$ should be approximately the same as those in purely hadronic collisions.[9,14] Since the inclusive charge density $d\langle Q\rangle/dy$ has been measured in pp and πp collisions we know what the situation is off of proton targets. Figure 5(a) from Ref. 19 shows $d\langle Q\rangle/dy$ determined from data on proton-proton collisions at the CERN ISR. Using Eq. (2.12) this can be integrated, as in Fig. 5(b), to give $\langle u(y)\rangle$ in these collisions. From the parton-model assumptions given above, the charge transfer in electroproduction is directly given by the probabilities $\rho_a(y)$,

$$\begin{aligned}
\langle u(y)\rangle^{\gamma^* p}|_{y<Y_h} = \tfrac{2}{3}[\rho_u(y) - \rho_{\bar{u}}(y)] - \tfrac{1}{3}[\rho_d(y) - \rho_{\bar{d}}(y)]\\
- \tfrac{1}{3}[\rho_s(y) - \rho_{\bar{s}}(y)].
\end{aligned} \tag{3.5}$$

This can be expressed, using (3.3), as

$$\langle u(y)\rangle^{\gamma^* p}|_{y<Y_h} = \tfrac{4}{3}v_u(y) - \tfrac{1}{3}v_d(y) \cong v(y), \tag{3.6}$$

where the approximate equality on the right-hand side has followed from assuming $v_u(y) = v_d(y) \equiv v(y)$, which looks like the corresponding Kuti-Weisskopf[20] parameterization for densities. This assumption is probably reasonable for y not too small. Thus to the extent that the charge transfer in hadronic collisions (for $y < \frac{1}{2}Y_{\max}$) given in Fig. 5(b) is equivalent to $\langle u(y)\rangle$ (for $y < Y_h$) in electroproduction (providing that the two experiments satisfy $\frac{1}{2}Y_{\max} = Y_h$), the probability $v(y)$ is shown directly in Fig. 5(b). Figure 6 illustrates a prediction for the charge density and charge transfer for electroproduction off of a proton target. For neutron targets, interchanging u and d subscripts in (3.3) gives a striking modification of (3.6),

$$\langle u(y)\rangle^{\gamma^* n}|_{y<Y_h} = \tfrac{2}{3}v_d(y) - \tfrac{2}{3}v_u(y) \cong 0, \tag{3.6'}$$

as illustrated in Fig. 7, with the associated hadronic collision prediction that charge transfer in πn should be approximately zero on the neutron side of the final-state rapidity plot. Any violation of this can be attributed to the breaking of the assumption that $v_d(y) \cong v_u(y)$.

At the point $y = Y_h$, the photon couples to a parton or antiparton. Because the "sea" is assumed composed of equal numbers of partons and antipartons and is therefore electrically neutral, charge is transferred on the average beyond this point in the diagram ($y > Y_h$) only if the photon couples to a valence quark. Therefore, if Y_h ($\approx \ln\omega$) is large enough so that $v(Y_h) \cong 0$ in Fig. 5(b) we expect a π^+/π^- charge ratio of unity, as

noted below (3.4). From Fig. 5(b) this occurs for $Y_h \cong 3$ ($\omega \cong 20$). If ω is small enough so that $v(Y_h)$ is not negligible, the spacelike photon can be thought of as transferring some of this (valence) charge to the parton fragmentation region. The exact manner in which this excess charge is distributed there depends on the details of the parton dynamics. The situation for $d\langle Q\rangle/dy$ and $\langle u(y)\rangle$ in electroproduction off protons is then something like what is pictured in Fig. 6. In the current plateau (CP), the charge transfer is approximately constant and equal to

$$\begin{aligned}\langle u(y)\rangle^{\gamma^* p}\,|_{y\in \mathrm{CP}} &= \tfrac{8}{27}[\rho_u(Y_h)-\rho_{\bar{u}}(Y_h)] \\ &\quad -\tfrac{1}{27}[\rho_d(Y_h)-\rho_{\bar{d}}(Y_h)] \\ &\quad -\tfrac{1}{27}[\rho_s(Y_h)-\rho_{\bar{s}}(Y_h)] \\ &= \tfrac{16}{27}v_u(Y_h)-\tfrac{1}{27}v_d(Y_h) \\ &\cong \tfrac{5}{9}v(Y_h). \end{aligned} \tag{3.7}$$

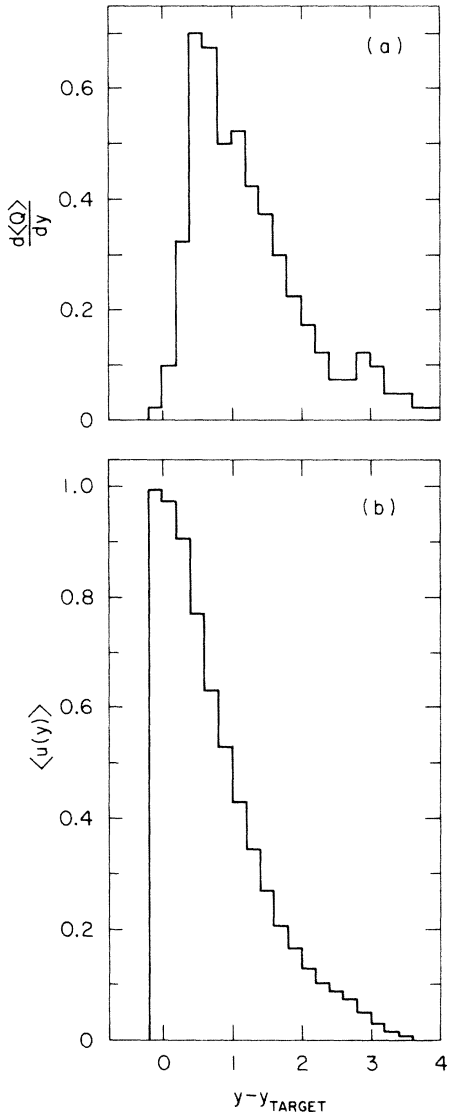

FIG. 5. Diagram (a) gives the rapidity charge density for scattering off a proton, determined from ISR data as discussed in Ref. 19. Diagram (b) gives the charge transfer $\langle u(y)\rangle$ across a given rapidity in pp collisions. From general Mueller-Regge arguments this should coincide with the charge transfer in $\gamma^* p$ collisions as long as we are in the NFR of the latter reaction. Assuming approximate equality of the distributions of u quarks and d quarks in the proton this is approximately $v(y)$, the probability that a particular valence quark in the quark-parton model is present at y.

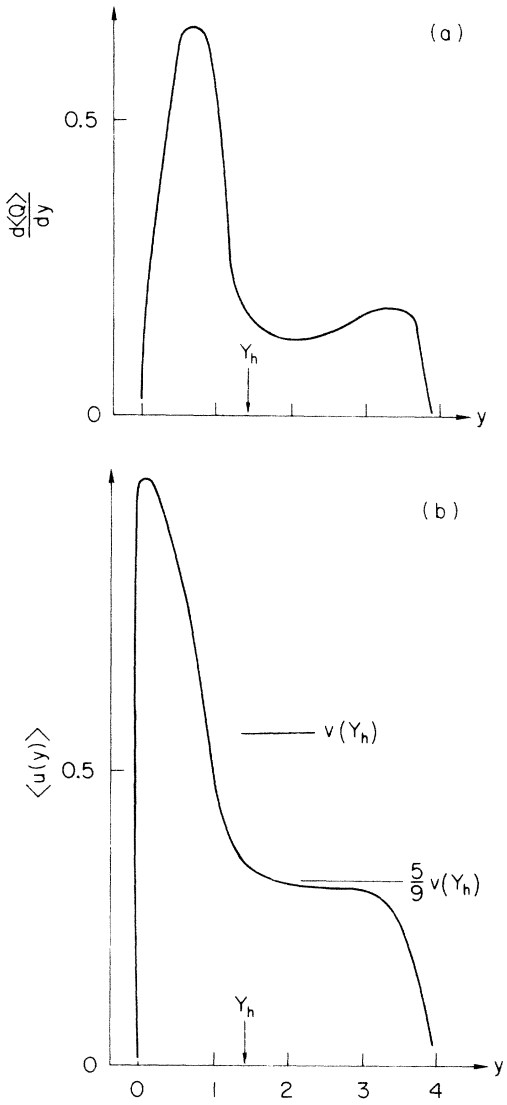

FIG. 6. Diagram (a) shows a prediction of the quark parton model for charge density in $\gamma^* p$ where $Y_h = \ln\omega \cong 1.4$. Diagram (b) shows the corresponding charge transfer. The charged transfer of $\frac{5}{9}v(Y_h)$ is appropriate to quark quantum numbers for the partons.

For electroproduction off of neutron targets, the distribution $v(Y_h)$ is assumed to coincide with Fig. 5(b) but the NFR is neutral because of cancellations between the one valence u quark and two valence d quarks. In the CP we have, using (3.7) and the quark composition of a neutron,

$$\langle u(y)\rangle^{\gamma^* n}\big|_{y\in \mathrm{CP}} = \tfrac{8}{27} v_u(Y_h) - \tfrac{2}{27} v_d(Y_h) \cong \tfrac{2}{9} v(Y_h), \qquad (3.7')$$

so that when the photon transfers charge out of the hole fragmentation region, charge conservation implies it should leave a negative charge density in HFR. The situation is shown in Fig. 7. In order to define just how big the HFR is, we note that it is possible to measure $d\langle Q\rangle/dy$ in γ^*-neutron final states and examine the region where the average density of charge is negative. In our picture this region should not extend all the way to $y_{\min}$ if ω is large enough. That is, it should be possible to partially separate the NFR and the HFR even at low ω.

Notice from the form of (3.7) and (3.7′) that the total charge transferred into the parton fragmentation region should depend only on $v(Y_h)$, the valence component, and not on the sea component $s(Y_h)$ and $s'(Y_h)$ as does the ratio $R(\pi^+/\pi^-)$. Comparing (3.7) and (3.7′) at different $Y_h \approx \ln\omega$ with the form of $v(y)$ determined separately in pp and πp collisions would provide a good test of these ideas. If this identification is not valid, then the assumption that the Mueller-Regge singularities in virtual-photon-induced reactions are similar to those in purely hadronic reactions could be questioned *or* the assignment of quantum numbers to the partons could be reconsidered. This assignment is disputable because of the anomalous behavior of $e^+e^- \to hX$.[2] If there were extra quark degrees of freedom (color, charm, etc.) not excited in electroproductions, it would still be possible that the simple fractional charge assignments would be valid. Equations (3.7) and (3.7′) should therefore be checked.

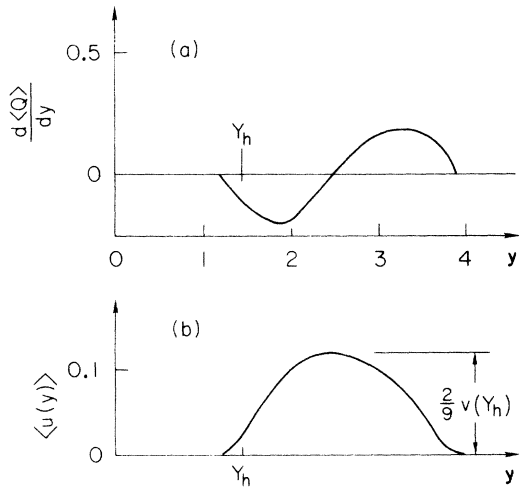

FIG. 7. Quark-parton model predictions for $\gamma^* n$ electroproduction. Diagram (a) gives charge density and (b) gives charge transfer.

Notice that we do not derive "sum rules" for the charge transfer $\langle u(y)\rangle$. These sum rules have been discussed in the context of the parton model by Hasenfratz.[21] The difference between his formalism and ours is that he deals with probability densities while we only consider straight probabilities.

Probably the most reasonable currently feasible test of Feynman's hypothesis[22] concerning the retention of some residual quark quantum numbers in the parton fragmentation region involves comparing (3.7) and (3.7′) with data, using the form $v(y)$ given in Fig. 5(b). In our model the baryon number of the quark is "screened" and does not necessarily show, so we do not implement the full content of Feynman's suggestion. When reliable studies can be made of inelastic νp or $\bar{\nu}p$ processes in the scaling limit, the selective action of neutrinos on d quarks ($d \to u$) and of antineutrinos on u quarks ($u \to d$) can be used to additionally sharpen our understanding of these regions in parton terms.

IV. BEHAVIOR OF $\langle u^2(y)\rangle$

In this section we shall see what kind of behavior to expect of $\langle u^2(y)\rangle$ in the important plateau regions HP and CP according to our model of electroproduction. Since this measurement only involves the counting of charged particles in a 4π detector with momentum resolution to divide the particles into two sets, $y_i < y$ and $y_j > y$, it is often easier to obtain than a two-particle correlation function, yet we will see that we can obtain some of the same information present in an inclusive correlation function by examining this quantity.

We shall first look at our model in the strong-ordering limit, in which $\langle u^2(y)\rangle$ may naturally tend to slightly different values in HP and CP. Then we shall examine the more interesting case where a breakdown of strong ordering occurs due to cluster formation, i.e., the (strong-ordered) production of excited states which subsequently decay (statistically), even possibly overlapping each other; the contribution of this process to the net $\langle u^2(y)\rangle$ is proportional to $d\sigma_{(1)}/dy$, and if there are subtle differences in the densities or clustering properties in the different kinematic regions, evidence may be seen here. This is an important

point, for although the Bjorken-Kogut correspondence principle[10] suggests that the dynamics in the five regions of Fig. 2 should be the same (implying,[9] e.g., $C_h = C_c$ in Fig. 2), there are reasons for believing otherwise, as we shall review.

There is an extreme case of cluster formation which we shall consider last: where the entire current side (CFR) of the process is one large cluster, or "fireball." For our purposes here we shall take CFR to be the region $Y_h < y < y_{\max}$. (The possibility that the hadron side of the electroproduction process could also be one large fireball has been effectively ruled out by the hadron-hadron collision studies[7] mentioned previously.) In Sec. IV D we shall discuss the usefulness of the semiexclusive quantity $\langle u^2(y)\rangle_n$, where n is the number of charged particles in CFR, i.e., having rapidity $y_i > Y_h$.

A. The strong-ordered limit

In the rigorous strong-ordering limit calculations on mean square charge transfer, at least in the plateau regions, are simple; in our one-dimensional quark-line diagrams, $\langle u^2(y)\rangle$ can be expressed in terms of the probabilities that various kinds of quark lines are cut when we separate the diagram into two pieces ($y_i < y$ and $y_i > y$). We are either cutting three quark lines (fermion exchange) or a quark and an antiquark (meson exchange):

$$\langle u^2(y)\rangle_{\rm MP} = \sum_{a,b,c} (Q_a + Q_b + Q_c)^2 p^F_{abc}(y) + \sum_{a,b} (Q_a - Q_b)^2 p^M_{a\bar b}(y), \tag{4.1}$$

where $p^F_{abc}(y)$ and $p^M_{a\bar b}(y)$ are the probabilities of finding those quark combinations at rapidity y. [The subscript MP signifies a pure (strong-ordered) multiperipheral-model result.]

In the HP where y is large enough so that the contribution from valence quarks in the proton can be neglected and the number of particles on each side of y is large, it makes sense to assume that the quark-line probabilities are independent,

$$p^F_{abc}(y) \to b(y) p_a p_b p_c\,, \qquad p^M_{a\bar b}(y) \to m(y) p_a p_b\,. \tag{4.2}$$

These equations are strictly valid only in the plateau region where $d\sigma_{(1)}/dy \to$ const. However, we want to allow for the continuation out of the plateau region and we make the assumption that (4.2) remains approximately valid, with

$$b(y) = b\left(\frac{d\sigma_{(1)}}{dy}\right)\Big/\left(\frac{d\sigma_{(1)}}{dy}\Big|_{\rm plateau}\right), \tag{4.3}$$

$$m(y) = m\left(\frac{d\sigma_{(1)}}{dy}\right)\Big/\left(\frac{d\sigma_{(1)}}{dy}\Big|_{\rm plateau}\right), \tag{4.4}$$

where $m = 1-b$ and $d\sigma_{(1)}/dy$ is the inclusive distribution of a *nonleading* particle. This can be considered a correction for "phase space" or "edge" effects leaving the independence of quark lines unchanged. This form can be justified by exchange-degeneracy arguments. In the limit of exact SU(3) we have [since y is large enough so that $v \cong 0$ in (3.3)]

$$p_u = p_d = p_s = \tfrac{1}{3}\,, \tag{4.5}$$

and (4.1) gives

$$\langle u^2(y)\rangle_{\rm MP} = \tfrac{2}{3}\, b(y) + \tfrac{4}{9} m(y) = \tfrac{4}{9} + \tfrac{2}{9} b(y)\,. \tag{4.6}$$

We can of course break SU(3) by taking $p_u = p_d = \frac{1}{2}(1-p_s)$, $p_s < \frac{1}{3}$. For example, if $p_s = 0$ then (for $y \in$ HP) $\langle u^2(y)\rangle = \frac{1}{2} b + \frac{1}{2}$, i.e., $\frac{1}{2} \leq \langle u^2(y)\rangle \leq 1$, but the important point is that $\langle u^2(y)\rangle_{\rm MP}$ *cannot* be larger than some number near unity in the quark model.

In the current plateau (CP) there is a charge-squared bias for one of the partons due to its interaction with the photon. For reasonably large $Y_h \sim \ln\omega$ (so we know the photon does not strike one of the proton's valence quarks), Eqs. (4.2) are replaced for CP by

$$\left.\begin{aligned} p^B_{abc}(y) &= \tfrac{2}{3} b'(y) p_a p_b Q_c^{\,2} \\ p^M_{a\bar b}(y) &= \tfrac{2}{3} m'(y) p_a Q_b^{\,2} \end{aligned}\right\}, \quad y \in {\rm CP} \tag{4.2'}$$

and we wind up, for perfect SU(3), with

$$\langle u^2(y)\rangle_{\rm MP} = \tfrac{7}{9} b'(y) + \tfrac{5}{9} m'(y) = \tfrac{5}{9} + \tfrac{2}{9} b'(y) \in \left(\tfrac{5}{9}, \tfrac{7}{9}\right) \tag{4.7}$$

again bounded by a number near unity for quark partons. We have primed the baryon and meson relative occurrences here to allow for the possibility that they are different from their HP counterparts in (4.3) and (4.4). In fact, comparison of (4.6) and (4.7) in this simple model shows that if $\langle u^2({\rm HP})\rangle = \langle u^2({\rm CP})\rangle$, then we *must* have different mixtures of baryons and mesons in the two regions.

Equations (4.6) and (4.7) should not be considered definitive predictions for $\langle u^2(y)\rangle$. They do give indication that this measurable may show some structure as we trace y across the available kinematic region. Important modifications due to clustering, which breaks the strong-ordering assumption, must be added. We now turn to investigate the extra contributions to $\langle u^2(y)\rangle$ from cluster formation.

B. Clustering included

Before treating electroproduction we shall review the evidence in favor of clustering in purely

hadronic collisions and the use of $\langle u^2 \rangle$ there in measuring its properties. Within the context of multiperipheral models, the necessity of production of clusters as well as individual hadrons has long been realized.[5,23] One simple way of seeing this has been pointed out by Henyey[24] and by Hamer and Peierls,[25] and is as follows. Viewed in impact-parameter space, a multiperipheral chain such as that drawn in Fig. 3 constitutes a random walk. The average step size, b_0, and the number of steps, m, then determine the mean spacing in impact parameter between the first and the last particle in the multiperipheral chain

$$\langle \Delta \vec{B}^2 \rangle \cong \langle m \rangle b_0^2 . \tag{4.8}$$

When inserted into the unitarity equation, (4.8) implies a relation between the logarithmic growth of average number of multiperipheral steps and the logarithmic shrinkage of the diffractive peak. Analysis suggests that these rates of growth are inconsistent unless particles are produced in clusters so that the number of steps,

$$\langle m \rangle = \langle N_{\text{clusters}} - 1 \rangle , \tag{4.9}$$

is less than the total number of particles.

Other calculations of multiplicity distributions, neutral charged multiplicity correlations, and correlation functions verify the necessity of clusters. The extensive analysis done by Berger and Fox[26] suggests that the average number of particles per cluster is between three and four, and then the mean spacing of clusters in rapidity is somewhat less than the spacing of the decay products of a single cluster. The connection between particles and clusters in the rapidity space of a typical event is then something like that shown in Fig. 8, taken from Ref. 6.

The presence of clusters means that we have to supplement the calculation of the mean square charge transfer of the simple nearest-neighbor multiperipheral model. A cluster produced at $\bar{y}_c > y$ can decay into stable charged particles, some of which have a finite probability of ending up with $y_i < y$. It is easy to see in a statistical treatment (say, where there is a binomial probability distribution for particles from a cluster produced at y to go left or right of y) that $\langle u^2(y) \rangle$ from a given cluster depends only on the shape of the single-particle distribution from the cluster; if several clusters $\{c\}$ (neutral on the average) are produced at different rapidities $\{y_c\}$ and decay independently, a random-walk treatment shows that $\langle u^2(y) \rangle_{\text{cluster}}$ is proportional to the density of clusters. [This is in contrast to $\langle u^2(y) \rangle_{\text{MP}}$ in (4.6) or (4.7), which was *independent* of the magnitude of the single-particle distribution, at least in the plateau region.] Quigg and Thomas[7] have calculated the contribution of cluster decay to $\langle u^2(y) \rangle$, assuming the production of neutral clusters of three particles, to be

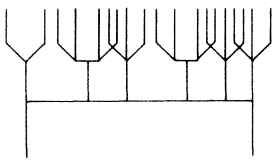

FIG. 8. Multiperipheral cluster model and origin of particles when cluster spacing in rapidity is of the same order as the size of a single cluster.

$$\langle u^2(y) \rangle_{\text{clusters}} = \tfrac{4}{3} \Delta(\sigma^{-1}) \frac{d\sigma_{(1)}}{dy}(y) , \tag{4.10}$$

where Δ is a parameter which measures the spacing in rapidity space of the particles from the decay. This parameter is separately measurable since, under the approximation of isotropic decay, Δ determines the width of the transverse momentum distribution. (Chao and Quigg[6] have also suggested studying correlations between n_L and n_R as a function of gap size between left and right hemispheres for an independent test of Δ.) The simple model of Quigg and Thomas is close enough to the average cluster properties determined empirically that we will take (4.10) to be a valid approximation of the charge-transfer effects of physical clusters.

When the clusters are not all neutral, the net $\langle u^2(y) \rangle$ is the sum of two terms:

$$\langle u^2(y) \rangle = \langle u^2(y) \rangle_{\text{MP}} + \langle u^2(y) \rangle_{\text{clusters}} , \tag{4.11}$$

where $\langle u^2(y) \rangle_{\text{MP}}$ reflects the contribution of the protoclusters given by Eq. (4.6) [$(y \in \text{HP})$] or Eq. (4.7) [$(y \in \text{CP})$] and $\langle u^2(y) \rangle_{\text{clusters}}$ by Eq. (4.10). We have assumed the average decay properties of the clusters to be independent of the charge transfers along the multiperipheral chain. The determination of Δ in (4.10) given by Bialas[27] indicates that the two terms in (4.11) are approximately equal for values of $(1/\sigma) d\sigma_{(1)}/dy$ typical of the plateau regions in hadronic reactions.

Making the aforementioned *ad hoc* modifications, (4.3) and (4.4), in the form of $\langle u^2(y) \rangle_{\text{MP}}$ to take "edge effects" into account, we find the prediction of the multiperipheral cluster model for the mean-square charge transfer in *hadronic* production processes is then

$$\langle u^2(y) \rangle \big|_{y \in \text{HP}} = \left[\left(\tfrac{4}{9} + \tfrac{2}{9} b \right) \left(\frac{d\sigma}{dy} \bigg|_{\text{HP}} \right)^{-1} + \tfrac{4}{3} \sigma^{-1} \Delta \right] \frac{d\sigma_{(1)}}{dy} , \tag{4.12}$$

where $d\sigma_{(1)}/dy$ is the inclusive cross section for a nonleading particle and the proportionality

constant now depends on both the multiperipheral Regge exchange and the cluster properties. Assuming approximate exchange degeneracy we get (4.6) to be valid in hadronic collisions, and inserting Bialas's value for Δ into (4.10) the prediction is

$$\langle u^2(y)\rangle \cong 0.8\,\frac{d\sigma_{(1)}^{\rm ch}}{dy}\,. \tag{4.13}$$

Figure 9 shows that this prediction gives a good description of data from K^-p and pp collisions. The agreement with (4.13) is quite good, and this implies that the properties of clusters are approximately energy-independent and roughly independent of the quantum number of the incident particles.

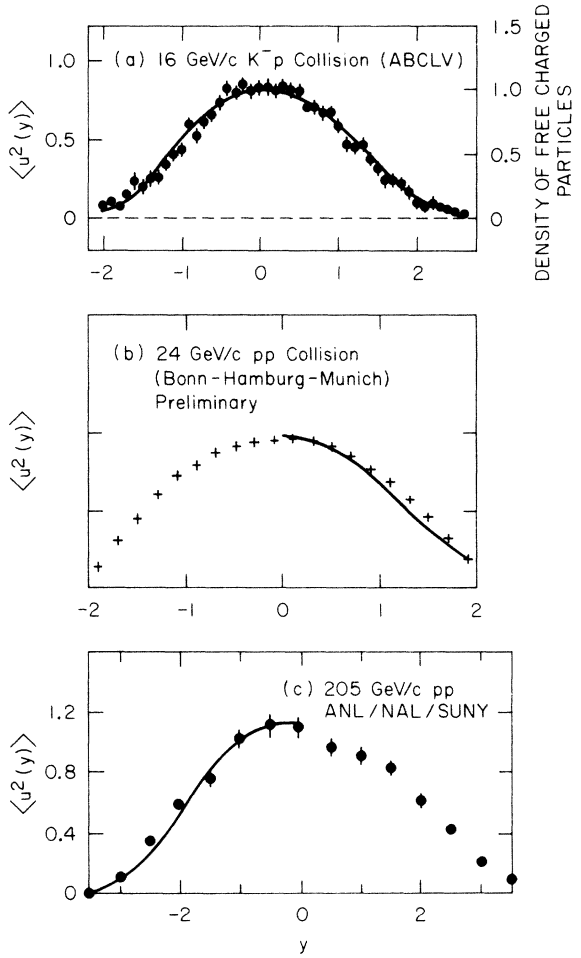

FIG. 9. Mean square charge transfer, $\langle u^2(y)\rangle$, in 16-GeV/c K^-p collisions, and 24-GeV/c and 205-GeV/c pp collisions, respectively. The diagrams are taken from Ref. 6. The curves are, respectively, $0.81 d\sigma_1^{\rm ch}/dy$, $0.85 d\sigma_1^{\rm ch}/dy$, and $0.72 d\sigma_1^{\rm ch}/dy$, where $d\sigma_1^{\rm ch}/dy$ is the single-particle density of a nonleading particle. The agreement with the multiperipheral cluster model (4.13) is quite good. See Chao and Quigg (Ref. 6) for further discussion.

C. Implications for electroproduction

Mueller-Regge analysis[14] or parton-model assumptions[9] imply that measurements on the final states of electroproduction in the nucleon fragmentation region (NFR) and the hadronic plateau (HP) must agree with the equivalent measurements in hadronic collisions. We can therefore expect that (4.13) should be true for $\langle u^2(y)\rangle$ in $\gamma^* p$, at least in these kinematic regions.

The validity of (4.13) over the entire kinematic range is quite another matter. We have already seen that the identification of the fundamental charged constituents with quarks leads to a discontinuity in $\langle u^2(y)\rangle_{\rm MP}$ between HP and CP calculated from the quark-line diagrams in Secs. III and IV. The difference between the hadronic sectors, Eq. (4.6), and the current sectors, Eq. (4.7), is not large, and given the fact that we have evidence (from hadronic collisions[7]) that this multiperipheral component is not the only contribution to $\langle u^2(y)\rangle$, it is not even necessarily detectable. However, there remains the possibility of dramatic dissimilarities between the clustering properties of hadrons in the PFR and those in the NFR. This contingency would conflict with the fundamental idea of the correspondence principle of Bjorken and Kogut[10] which suggests that all properties of final-state hadrons are the same in the entire kinematic region, but there are some simple intuitive reasons for considering the possibility.

One of the reasons we might expect different clustering in the PFR has to do with the space-time evolution of a deep-inelastic interaction in the quark-parton model. As has been frequently discussed, the fact that free quarks are not observed in deep-inelastic processes puts severe constraints on the forces which bind partons to form hadrons. If the forces were such that only short-range correlations in rapidity space were present, then the large rapidity gap between the initial and the final location of the struck parton in Fig. 3 would not allow the other quarks to arrange themselves in such a way that the only particles are of zero triality.[28] Some *ad hoc* evasions of this difficulty have been proposed.[29] A study by Casher, Kogut, and Susskind[30] of a soluble two-dimensional model of spinor electrodynamics indicates that it is possible to have a causal explanation of this type of "screening" of the quark quantum numbers. The CFR hadrons in Fig. 3 are created in a kind of "inside-outside" cascade of vacuum polarization in this view of deep-inelastic processes, and therefore the "condensation" of quark-antiquark pairs to form hadrons or clusters of hadrons should arise from

a different principle in CFR than in hadronic collisions, where there are several indications of short-range order. The fact that the cluster properties in hadronic collisions appear to be roughly independent of target and energy gives some indication that *hadronic* dynamics demonstrates a form of universality. If clustering arises in the dynamics a different kind of clustering should be taking place in CFR.

Another reason for expecting different clustering phenomena in deep-inelastic interactions can be found in the interpretation of data on e^+e^- annihilations at SPEAR. Preliminary measurements on this reaction which is closely related to the CFR in deep-inelastic electroproduction indicate that[2]

$$\langle n_0\rangle_{e^+e^-} \cong \langle n_{\rm ch}\rangle_{e^+e^-} , \tag{4.14}$$

in striking contrast to the situation in hadronic collisions,[5]

$$\langle n_0\rangle_h \cong \tfrac{1}{2}\langle n_{\rm ch}\rangle_h . \tag{4.15}$$

Cluster models have shown the ability to deal with multiplicity correlations such as $\langle n_0\rangle_{n_-}$ vs n_-,[31] but the identification of clusters with ordinary hadronic resonances argues against a traditional clustering explanation of (4.14).

The possibility, then, looms large for divergence from the Bjorken-Kogut correspondence result that (4.13) is valid for electroproduction over the entire range of kinematically accessible variables. The opportunity exists for the detection of an exciting new class of clustering phenomena. Since the measurement of $\langle u^2(y)\rangle$ is comparatively easy, the experimental check of these possibilities should take place soon. For example, a possible result is pictured in Fig. 10 which was drawn assuming larger-mass clusters in CFR with the properties of these clusters being energy-independent.

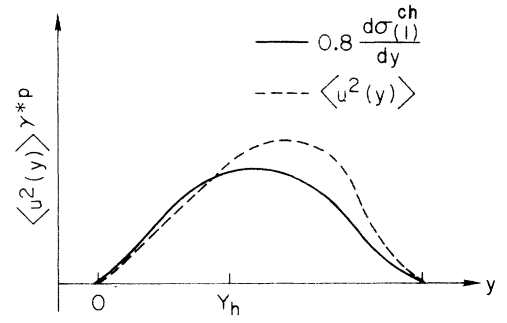

FIG. 10. Hypothetical deviation from (4.13) in γ^*p electroproduction attributable to heavy-mass clusters in the current fragmentation region.

D. Extreme case: Fireball in current fragmentation region (CFR)

In a previous paper[8] we have proposed that measurements of mean-square charge transfer should be able to decide between an underlying parton approach and a "statistical fireball" approach to e^+e^- annihilation. Because the mechanism of annihilation should be reflected in the CFR of the electroproduction final state,[9] it would seem reasonable that similar searches could be conducted there. We have already noted that the existence of a single large fireball is not expected on the hadron side, since the data must coincide with hadronic collisions where strong evidence for short-range order is already known.[7]

It is now simple to take account of this contingency, since a fireball is only a large cluster, having, say, n charged fragments. However, our treatment of clusters in the previous subsection assumed that each cluster always had close to some average number of decay products (i.e., the individual dispersions in number of decay products were small), whereas we must relax this restriction for fireballs. Thus, in looking at fireball mechanisms, we must separate the events into categories labeled by the number of charged final-state particles; this was the technique used in Ref. 8.

For illustration we consider the set of events in whose final states there are n_c charged particles in CFR. These n_c particles are hypothetically assigned to a current fireball having n_c charged decay products, and measurements are made of $\langle u^2(y)\rangle_{n_c}$ for $y\in(Y_h, y_{\rm max})$. To simplify matters as much as possible, we shall first ignore all particles on the hadron side ($y_i < Y_h$), and take the current fireball to be neutral; necessary modifications of the results so obtained will be easily made by a random-walk method outlined later.

Consider a given final state which has n_L charged particles in the "left" range (Y_h, y) and n_R charged particles in the "right" range $(y, y_{\rm max})$. We will assume for convenience that all charged particles are singly charged. Since only over-all charge conservation is in force and not semilocal charge conservation, we have large possible fluctuations of charge transfers in CFR,

$$(|u(y)|_{n_c})_{\rm max} = \min(n_L, n_R) , \tag{4.16}$$

and the observation of $|u(y)|_{n_c} \gg 1$ in any event points to the existence of a large current fireball.

Let $P^y_{n_+}(n_{R+}, n_{R-})$ be the probability that a final state with n_+ positive (and so by assumed neutrality of CFR $n_- = n_+$ negative) particles should send n_{R+} positive and n_{R-} negative particles into

the right range, i.e., to the right of rapidity y in CFR. If we assume independence of positive and negative particle motions in CFR, then

$$P^y_{n_+}(n_{R+}, n_{R-}) = P^y_{n_+}(n_{R+}) P^y_{n_+}(n_{R-}) \ . \tag{4.17}$$

This assumption should be good for $\ln s \gg \omega \gg 1$ where the CFR is large and particles therein are produced copiously; in any case it is the best we can do in a simple model. Momentum and charge conservation may make some corrections when $n_{R+} \approx 0$ or n_+, but we will assume that these configurations are negligible (except near $y_{\max}$, but we will ignore this difficulty for simplicity). We then have

$$\langle u^2(y)\rangle_{n_+} = \sum_{n_{R+}} P^y_{n_+}(n_{R+}, n_{R-})(n_{R+} - n_{R-})^2$$
$$\equiv 2\left[\langle n_{R+}{}^2\rangle_{n_+} - \langle n_{R+}\rangle_{n_+}{}^2\right]. \tag{4.18}$$

For example, let $P^y_{n_+}(n_{R+})$ be of binomial distribution form,

$$P^y_{n_+}(n_{R+}) = r_+{}^{n_{R+}}(y)\, l_+{}^{n_{L+}}(y) \binom{n_+}{n_{R+}} \ , \tag{4.19}$$

where $r_+(y) = 1 - l_+(y)$ is the probability for a positively charged particle to go to the right of rapidity y. For $Y_c \gg 1$ (where CP dominates the CFR) and assuming a flat plateau, we take

$$l_+(y) = \frac{y - Y_h}{Y_c} \quad \text{for } y \in \text{CFR} \ . \tag{4.20}$$

Then using C invariance [which requires $l_+(y) = l_-(y)$ and $r_+(y) = r_-(y) = 1 - l_+(y)$] we have

$$\langle u^2(y)\rangle_{n_+} = 2n_+ l_+(y)[1 - l_+(y)] \ . \tag{4.21}$$

Thus we see a fundamental difference between the strongly ordered MPM of Sec. IV A, or even the mildly ordered multiperipheral model of Sec. IV B, and the unordered fireball model: In the former two, $\langle u^2(y)\rangle_{n_c}$ is finite and roughly independent of n_c; in the latter it grows with (charged) multiplicity without limit.

Generalizations of the remarks above lead to the result that $\langle u^2(y)\rangle_{n_c}$ in a one-fireball model (as opposed to a several-cluster model in which all clusters have the same multiplicity) depends only on the shape of the over-all fireball multiplicity distribution $d\sigma^{\rm ch}_{(1)}/dy$. In Sec. IV B, we saw that random-walk arguments implied that if several independent fireballs (or clusters, *including* single-particle clusters) were involved in a given event, then the net $\langle u^2(y)\rangle_{n_c}$ for the process was simply the sum of the individual $\langle u^2(y)\rangle_{n_c}$ of the individual fireballs. This makes it easy to write down the net $\langle u^2(y)\rangle_{n_c}$ for a given event in electroproduction even when the underlying mechanisms involved in the hadron side and the current side are different, and also to include the possibility of the CFR fireball not being over-all neutral. The behavior of $\langle u^2(y)\rangle_{n_c}$ for a pure fireball is shown in Fig. 11. This should be compared with the forms obtained in a strong-ordered limit and in the finite (energy-independent) size cluster limit.

V. SUMMARY

Tests of the quark-parton model in electroproduction, where it has already experienced some success, are all the more crucial now in view of the new e^+e^- annihilation data[2] which seem to strike at its roots. In this paper we have urged probing electroproduction mechanisms by measuring charge transfer and fluctuations in the hadronic final states of deep-inelastic electroproduction, and have also presented sample predictions based on simple parton pictures. The experimental measurements we have proposed are easily done and have important implications within the context of the standard models we considered. These measurements consist in determining $\langle u(y)\rangle$, $\langle u^2(y)\rangle$, and $\langle u^2(y)\rangle_{n_c}$ for large-s events having various given ω's, where n_c is the charged multiplicity in CFR ($y > Y_h \cong \ln\omega$).

The behavior of $\langle u^2(y)\rangle_{n_c}$ depends critically on the

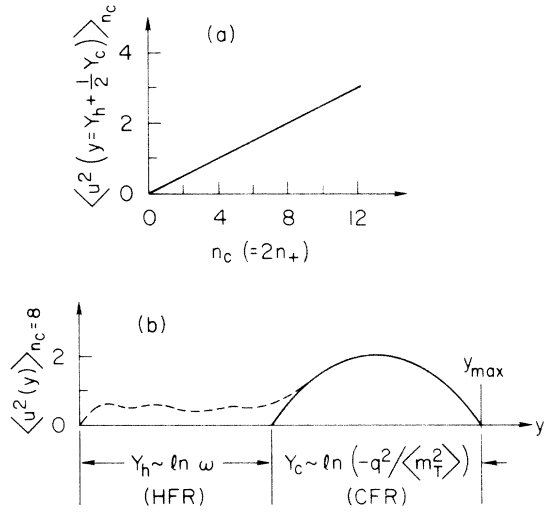

FIG. 11. This figure illustrates the behavior of $\langle u^2(y)\rangle_{n_c}$ in CFR ($Y_h < y < y_{\max} = Y_h + Y_c$) in the extreme case that CFR consists of one fireball of charge multiplicity n_c ($= 2n_+ = 2n_-$). We have assumed Y_c to be large enough that a flat plateau dominates CFR, and have used Eq. (4.21) with (4.20). Diagram (a) shows $\langle u^2(y)\rangle_{n_c}$ vs n_c across y *fixed* in the center of CFR [so $l_+ = \frac{1}{2}$ in (4.21)]. Diagram (b) shows $\langle u^2(y)\rangle_{n_c}$ vs y for n_c, the CFR charged multiplicity, *fixed* at 8. To the extent that charge distributions in HFR and CFR are independent of each other, the net $\langle u^2(y)\rangle$ represented by the dashed line in (b) is the sum of the $\langle u^2(y)\rangle$'s for each region separately, as indicated.

clustering properties in CFR—it is near unity for *all* n_c if individual cluster size is limited and energy-independent. This is already thought to be the case in hadronic production processes where $\langle u^2(y)\rangle$ and $\langle u^2(y)\rangle_n$ are identical. On quite general grounds it should therefore be true in the hadronic regions of inelastic electroproduction. If the cluster size in the CFR is not so limited, $\langle u^2(y)\rangle_{n_c}$ behaves as depicted in Fig. 11.

Even if energy independence of clustering is established, the usefulness of $\langle u^2(y)\rangle$ is not exhausted. For example, it can be used to test the Bjorken-Kogut correspondence principle,[10] which suggests that characteristics of the electroproduction final states should not vary radically between different kinematic regions. A simple extension of their discussion is that clustering properties of hadrons should be the same in the current fragmentation region as in the target fragmentation region. We have presented some simple intuitive arguments why this may not be so, and then have shown how measurements of $\langle u^2(y)\rangle$ can provide a sensitive test of this hypothesis; cf. Eqs. (4.6) and (4.7).

Regardless of how the clustering properties reveal themselves in $\langle u^2\rangle$ measurements, the microscopic structure of our model can still be probed. For example, particle ratios in the CFR have been measured and provide qualitative support for quark-parton ideas. A more quantitative test of the assignment of quark quantum numbers to the constituent partons can be formulated in terms of $\langle u(y)\rangle$, the charge transfer across a given rapidity, in Eqs. (3.6) and (3.7) for HFR and CFR respectively, in terms of $v(y)$ and $v(y)|_{y=Y_h}$, the probability that a particular valence quark is present at rapidity y. This probability can be separately determined by the charge transfer in high-energy proton-proton collisions.[7,9]

---

*Work supported by the U. S. Atomic Energy Commission.

[1]R. P. Feynman, *Photon Hadron Interactions* (Benjamin, New York, 1972); S. M. Berman, J. D. Bjorken, and J. B. Kogut, Phys. Rev. D 4, 3388 (1971); S. D. Drell and T.-M. Yan, Phys. Rev. Lett. 24, 855 (1970); J. D. Bjorken, Phys. Rev. D 7, 282 (1973); H. J. Lipkin and E. A. Paschos, Phys. Rev. Lett. 29, 525 (1972).

[2]B. Richter, talk presented at the Irvine Conference on Lepton-Induced Reactions, 1973 (unpublished).

[3]M. Chaichian, S. Kitakado, S. Pallua, and Y. Zarmi, Nucl. Phys. B58, 140 (1973); M. Chaichian, S. Kitakado, W. S. Lam, and Y. Zarmi, Nucl. Phys. B61, 77 (1973); M. Chaichian, S. Kitakado, W. S. Lam, and Y. Zarmi, Univ. of Helsinki Report No. 21-73 (unpublished).

[4]For a review of multiperipheral models see W. R. Frazer, L. Ingber, C. H. Mehta, C. H. Poon, D. Silverman, K. Stowe, P. D. Ting, and H. J. Yesian, Rev. Mod. Phys. 44, 284 (1972).

[5]For a review of the evidence for clustering, see S. Pokorski and L. Van Hove, CERN Report No. CERN TH 1772 (unpublished).

[6]A. W. Chao and C. Quigg, Phys. Rev. D 9, 2016 (1974).

[7]S. Nussinov, C. Quigg, and J.-M. Wang, Phys. Rev. D.6, 2713 (1972); T. T. Chou and C. N. Yang, *ibid.* 7, 1425 (1973); C. Quigg and G. H. Thomas, *ibid.* 7, 2752 (1973); D. R. Snider, *ibid.* 7, 3517 (1973); D. Sivers and G. H. Thomas, *ibid.* D 9, 208 (1974); D. Sivers, in *Particles and Fields–1973,* proceedings of the 1973 Meeting of the Division of Particles and Fields of the APS, Berkeley, California, edited by H. H. Bingham, M. Davier, and G. R. Lynch (AIP, New York, 1973).

[8]J. L. Newmeyer and Dennis Sivers, Phys. Rev. D 9, 2592 (1974).

[9]J. D. Bjorken, Phys. Rev. D 7, 282 (1973); R. N. Cahn, J. W. Cleymans, and E. W. Colglazier, Phys. Lett. 43B, 323 (1973).

[10]J. D. Bjorken and J. Kogut, Phys. Rev. D 8, 1341 (1973); J. Kogut, *ibid.* 8, 3029 (1973).

[11]For a simple introduction to the kinematics in electroproduction, see M. Perl, in the Proceedings of the Stanford Linear Accelerator Center Summer Institute on Particle Physics, 1973 (unpublished).

[12]See, for example, Perl, Ref. 11, or M. L. Perl, in *Proceedings of the XVI International Conference on High Energy Physics, Chicago-Batavia, Ill., 1972,* edited by J. D. Jackson and A. Roberts (NAL, Batavia, Ill., 1973), Vol. 2, p. 83.

[13]G. Miller *et al.*, Phys. Rev. D 5, 528 (1972); see also A. Bodek *et al.*, in *Particles and Fields–1973,* proceedings of the 1973 Meeting of the Division of Particles and Fields of the APS, Berkeley, California, edited by H. H. Bingham, M. Davier, and G. R. Lynch (AIP, New York, 1973).

[14]R. N. Cahn and E. W. Colglazier, Phys. Rev. D 8, 3019 (1973). [A proof of the equivalence of multiperipheral and Mueller-Regge pictures has been given by S. Pinsky, D. Snider, and G. Thomas, Phys. Lett. 47B, 505 (1973).

[15]See also J. T. Dakin and G. J. Feldman, Phys. Rev. D 8, 2862 (1973) and Refs. 5–8 (data) therein; F. J. Gilman, in proceedings of the Irvine Conference on Lepton-Induced Reactions, 1973 (unpublished).

[16]See, for example, C. E. DeTar, Phys. Rev. D 3, 128 (1971).

[17]H. Harari, Phys. Rev. Lett. 22, 562 (1969); J. L. Rosner, *ibid.* 22, 689 (1969).

[18]W. S. Lam, J. Tran Thanh Van, and I. Uschersohn, Rutherford report, 1973 (unpublished).

[19]D. Sivers, Phys. Rev. D 8, 2272 (1973).

[20]J. Kuti and V. Weisskopf, Phys. Rev. D 4, 3418 (1971).

A distribution which more faithfully reproduces F^{en}/F^{ep} data has been given by R. McElhaney and S. F. Tuan, Phys. Rev. D 8, 2267 (1973).
[21]P. Hasenfratz, Phys. Lett. 47B, 60 (1973).
[22]R. P. Feynman in Ref. 1, Appendix A. For counter-examples to this proposal, see G. R. Farrar and J. L. Rosner, Phys. Rev. D 7, 2747 (1973), or R. N. Cahn and E. W. Colglazier, Phys. Rev. D 9, 2658 (1974).
[23]See, for example, C. J. Hamer, Phys. Rev. D 7, 2723 (1973).
[24]F. Henyey, Phys. Lett. 45B, 363 (1973).
[25]C. J. Hamer and R. F. Peierls, Phys. Rev. D 8, 1358 (1973).
[26]E. L. Berger and G. C. Fox, Phys. Lett. (to be published).
[27]A. Bialas, CERN Report No. CERN-TH-1745 (unpublished).
[28]J. Kogut, D. Sinclair, and L. Susskind, Phys. Rev. D 7, 3637 (1973); 8, 2746(E) (1973).
[29]J. D. Bjorken, in proceedings of the Stanford Linear Accelerator Center Summer Institute on Particle Physics, 1973 (unpublished).
[30]A. Casher, J. Kogut, and L. Susskind, Phys. Rev. Lett. 30, 792 (1973).
[31]E. L. Berger, D. Horn, and G. H. Thomas, Phys. Rev. D 7, 1412 (1973); D. Horn and A. Schwimmer, Nucl. Phys. B52, 221 (1973).

PHYSICAL REVIEW D VOLUME 10, NUMBER 1 1 JULY 1974

Parity violation in deep-inelastic charged lepton-hadron scattering*

Warren J. Wilson
Jefferson Physical Laboratory, Harvard University, Cambridge, Massachusetts 02138
(Received 3 January 1974)

The possibility of detecting parity violation in deep-inelastic charged lepton-hadron scattering using polarized lepton beams is discussed. Assuming scaling, the quark-parton picture of the nucleon, and some general features of the weak currents, a general formula for the size of the parity-violating effect is derived. Specific estimates are made for various spontaneously broken gauge-symmetry models of the weak and electromagnetic interactions.

I. INTRODUCTION

Recent experimental evidence[1] for the existence of neutral weak currents in neutrino-hadron scattering has renewed interest in the question of whether such currents can produce measurable effects in charged lepton-hadron reactions. It has been pointed out that since the new currents are, in general, parity-violating, they should be detectable by an asymmetry in the inclusive cross sections for beams[2] (or targets[2,3]) polarized parallel and antiparallel to the lepton beam momentum. In this paper this asymmetry is estimated using the quark-parton model and some very general assumptions about the neutral weak currents. The general result is then specialized to some specific models, including those of Weinberg[4] and Salam[5] (WS) and Lee,[6] Prentki, and Zumino[7] (LPZ). This calculation is similar to that of Derman,[2] who did the calculation in the WS model in the case where the Weinberg angle, θ_W, is zero. It is the purpose of this paper to show that the size of the asymmetry is very sensitive to the parameters of the model being used. In fact, in the WS model, for values of θ_W near $\sin^2\theta_W = 0.3$, the asymmetry is expected to be an order of magnitude less than Derman's estimate.

II. THE CALCULATION

The process of interest is shown schematically in Fig. 1. For simplicity, the lepton beam is taken to be completely polarized either parallel or antiparallel to the beam direction (helicity, $\lambda = \pm 1$). Also, the kinematic variables are assumed to be in a region where the hadronic structure functions exhibit scaling, and it is appropriate to use the parton model to calculate them. In the general context of spontaneously broken gauge theories, the electromagnetic currents interact via the exchange of virtual photons, and the weak neutral currents by exchanging virtual Z mesons. To lowest order in weak and electromagnetic coupling constants, the parton picture of the reaction therefore appears as in Fig. 2. The form of the electromagnetic currents is assumed known:

$$J_\mu^l = -\bar{l}\gamma_\mu l\,, \qquad J_\mu^h = \sum_i Q_i\,\bar{q}_i\,\gamma_\mu\,q_i\,, \tag{1}$$

where the sum is over quark types and Q_i is the charge of the i-type quark. The neutral currents have the general form